




RESEARCH ARTICLE

The ABC transporter family efflux pump PvdRT-OpmQ of *Pseudomonas putida* KT2440: purification and initial characterization

 Nicola Victoria Stein¹ , Michelle Eder¹ , Sophie Brameyer^{1,2} , Serena Schwenkert³  and Heinrich Jung¹ 
¹ Microbiology, Faculty of Biology, Ludwig Maximilians University Munich, Martinsried, Germany

² Service Unit Bioanalytics, Faculty of Biology, Ludwig Maximilians University Munich, Martinsried, Germany

³ Service Unit Mass Spectrometry of Biomolecules, Faculty of Biology, Ludwig Maximilians University Munich, Martinsried, Germany

Correspondence

 H. Jung, Division of Microbiology, Faculty of Biology, Ludwig Maximilians University Munich, D-82152 Martinsried, Germany
 Tel: +49 89 2180 74630
 E-mail: hjung@lmu.de

(Received 30 November 2022, revised 31 January 2023, accepted 6 February 2023, available online 28 February 2023)

doi:10.1002/1873-3468.14601

Edited by Peter Brzezinski

Tripartite efflux systems of the ABC-type family transport a variety of substrates and contribute to the antimicrobial resistance of Gram-negative bacteria. PvdRT-OpmQ, a member of this family, is thought to be involved in the secretion of the newly synthesized and recycled siderophore pyoverdine in *Pseudomonas* species. Here, we purified and characterized the inner membrane component PvdT and the periplasmic adapter protein PvdR of the plant growth-promoting soil bacterium *Pseudomonas putida* KT2440. We show that PvdT possesses an ATPase activity that is stimulated by the addition of PvdR. In addition, we provide the first biochemical evidence for direct interactions between pyoverdine and PvdRT.

Keywords: ABC transporter; ligand binding; membrane protein purification; pyoverdine; siderophore; tripartite efflux pump

Iron is essential for almost every organism since it is involved in numerous metabolic processes. It is crucial for oxygen transport by hemoglobin and the conversion of energy during electron transfer in the respiratory chain. It functions as a cofactor of enzymes involved in DNA replication and metabolic pathways like the aconitase and the succinate dehydrogenase of the citric acid cycle [1,2], and it is crucial for host-pathogen interactions [3]. Ferrous (Fe^{2+}) ions are soluble and can be transported into cells by iron-specific transporters. However, ferrous ions are easily oxidized under aerobic conditions to ferric (Fe^{3+}) ions leading to the formation of hardly soluble polymeric ferric hydroxides [4]. In order to use ferric ions, pro- and eukaryotes (fungi, plants) produce and secrete

siderophores, organic compounds that chelate these ions and bring them into solution [5]. Fluorescent pseudomonads produce the siderophore pyoverdine (Fig. S1A), a polypeptide linked to a dihydroxyquinoline chromophore [6]. Synthesis and transport of pyoverdine across cell membranes are controlled by the ferric uptake regulator (Fur) via specific σ -factors [7,8].

To secrete siderophores into the environment, Gram-negative bacteria use tripartite efflux systems [9–12]. These systems consist of three major components: an inner membrane protein, which binds the substrate and drives secretion by either hydrolyzing ATP (ATP binding cassette (ABC) type efflux systems) or utilizing the proton motive force (e.g., RND-type efflux systems), a periplasmic adapter protein and an outer

Abbreviations

ABC transporter, ATP-binding cassette transporter; AP, alkaline phosphatase; BSA, bovine serum albumin; DDM, n-dodecyl- β -D-maltopyranoside; DRaCALA, differential radial capillary action of ligand assay; LC-MS/MS, liquid chromatography–tandem mass spectrometry; LDAO, dodecyltrimethylammonium oxide; NTA, nitrilotriacetic acid; OD, optical density; RT, room temperature; SPR, surface plasmon resonance; TBS, Tris-buffered saline; TM, transmembrane domain.

membrane porin. The periplasmic adaptor protein forms a tunnel that connects the inner and outer membrane proteins [13,14]. MacAB-TolC of *Escherichia coli* is a well-characterized example of a tripartite efflux pump of the ABC type, which is involved in drug resistance. The inner membrane component MacB consists of an N-terminal nucleotide-binding domain (NBD) located on the cytoplasmic side of the membrane, four transmembrane domains (TMs), and a periplasmic domain formed by the loop between TMs I and II involved in substrate binding [15]. MacB forms a dimer that couples ATP binding and hydrolysis by the NBD with periplasmic conformational changes that deliver substrates from the periplasm to the extracellular space *via* the adaptor protein MacA and the outer membrane protein TolC [15]. Previous analyses using purified proteins have shown that MacA stimulates the ATPase activity of MacB [14].

Analyses of *Pseudomonas aeruginosa* suggest that the ABC-type tripartite efflux system PvdRT-OpmQ contributes to the secretion of the newly synthesized and recycled siderophore pyoverdine [10,11]. This system shows high sequence similarity (> 60% identical amino acids) to PvdRT-OpmQ of the soil bacterium *P. putida* KT2440. Deletion of this system in both *Pseudomonas* strains impaired strain growth under iron-limited conditions and reduced secretion of the siderophore but never abolished it completely [12,16]. In addition to the PvdRT-OpmQ system, the RND-type tripartite efflux system MdtABC-OpmB was proposed to participate in pyoverdine secretion of *P. putida* KT2440 [12]. Upon deletion of both transport systems, secretion into the medium was reduced to 34% of the wild-type level, suggesting the participation of at least one more system. In addition, the mutant accumulated significantly more fluorescent siderophores in the periplasm [12]. Similar results were obtained for the secretion of enterobactin in *E. coli*, in which three different systems are involved. Here, even the deletion of all three systems could not completely abolish the secretion of enterobactin [9]. In addition, the type VI secretion system (T6SS) [17] and other tripartite efflux systems, such as MexAB-OprM [16] from *Pseudomonas*, have been proposed to be pyoverdine transporters, but not all could be confirmed. Therefore, the investigation of the pyoverdine circuit in fluorescent pseudomonads is still ongoing [18]. Although much is known about the transport [10,12], recycling [11], and synthesis pathways of [4,19], biochemical evidence for interactions between the tripartite efflux systems of *Pseudomonas* species with pyoverdine is not yet available. Since even a double deletion of both systems ($\Delta pvdRT\text{-}opmQ \Delta mdtA$) did not eliminate the secretion of the siderophore, further investigation and

proof of substrate binding would deepen the understanding of the functionality of this circuit in pseudomonads.

Here, we set out for an initial biochemical characterization of PvdRT of *P. putida* KT2440. We purified PvdR and PvdT to perform biochemical assays. First, the binding of pyoverdine to these proteins was shown. Second, the ATPase activity of PvdT and the influence of PvdR and pyoverdine on this activity were analyzed. The results revealed that pyoverdine indeed interacts with the PvdRT complex. In addition, PvdT was shown to hydrolyze ATP, and PvdR stimulated the reaction.

Material and methods

Cultivation

Escherichia coli and *P. putida* strains and plasmids used for this investigation are listed in Tables S1 and S2. Cells were cultivated aerobically by constant shaking at 180 rpm at 37 or 30 °C, respectively. Cells transformed with plasmids were grown in the presence of kanamycin (50 $\mu\text{g}\cdot\text{mL}^{-1}$). Gene expression was induced with 1 mM anthranilic acid. For all cultivation steps, LB medium was used (1% tryptone/peptone, 1% NaCl, 0.5% yeast extract). For agar plates, the medium was supplemented with 1.5% agar and poured into Petri dishes. Plates were incubated at 30 °C and, after colony growth, stored at 4 °C.

Cloning

For overproduction and purification of PvdT, the gene was cloned into pUCP20-ANT2-MCS [20] using the multiple cloning site and restriction enzymes. Additionally, the sequence encoding a SUMO tag was amplified from a pET-SUMO system from Thermo Fisher. During amplification by PCR, a histidine tag (7His) and a glycine-serine (G-S) linker were added to the SUMO tag by primers. All fragments were cloned into pUCP20-ANT2-MCS [20] yielding plasmid pUCP20-ANT2-7His-SUMO-pvdT using the restriction enzymes *Bam*HI and *Nde*I for the 7His-SUMO tag. For the *pvdT* amplicon, restriction enzymes *Nde*I and *Xba*I were used, respectively. For overproduction and purification of PvdR, the gene was amplified and subsequently cloned into pUCP20-ANT2-*hutT* [21], yielding plasmid pUCP20-ANT2-*pvdR6His*. Amplicons were digested using restriction enzymes *Nde*I and *Xho*I. Extraction of DNA fragments from agarose gels was performed using HiYield[®] PCR Clean-up/Gel extraction Kit (SLG[®]). Digested and purified amplicons were ligated using T4 DNA ligase, and *E. coli* DH5 α was transformed with respective plasmids. Plasmids were extracted from overnight cultures in LB supplemented with kanamycin (50 $\mu\text{g}\cdot\text{mL}^{-1}$) using the

HiYield® Plasmid Mini Kit (SLG®). Plasmids, respective strains, and primers can be found in Tables S1–S3.

Protein purification

Pseudomonas putida KPI with pUCP20-ANT2-7His-SUMO-pvdT and *P. putida* KT2440 pUCP20-ANT2-pvdR-6His were grown aerobically in LB medium at 30 °C. Gene expression was induced by adding 1 mM anthranilic acid at OD₆₀₀ = 0.55, and cultivation was continued for 3 h. Cells were harvested and washed with 50 mM Tris/HCl pH 8.0, after which cells were shock frozen in liquid nitrogen and stored at –80 °C until further use. All the following steps were carried out at 4 °C or on ice. The cells were thawed and resuspended in 50 mM Tris/HCl pH 8.0, 100 mM KCl, supplemented with protease inhibitor Pefabloc at a concentration of 0.2 mg·mL⁻¹, and disrupted with high pressure (1.35 kbar) in a Constant Cell Disruptor. Unbroken cells and debris were removed by centrifugation (4500 g, 30 min). Membranes were collected by centrifugation at 235 000 g for 1.5 h. Resulting membranes were washed and resuspended in a small buffer volume, frozen in liquid nitrogen, and stored at –80 °C. The Peterson protein assay was performed to determine the concentration of proteins in the membranes [22]. For protein purification, membranes (5 mg·mL⁻¹ total membrane protein) were solubilized during stirring for 90 min with either 1.5% lauryldimethylamine oxide (LDAO) for 7His-SUMO-PvdT containing membranes or 2% n-dodecyl-β-D-maltopyranoside (DDM) for membranes harboring PvdR6His in 50 mM Tris/HCl pH 8.0 containing 10 mM imidazole, 300 mM KCl and 5% [for surface plasmon resonance (SPR) measurements] or 10% glycerol (for ATPase measurements). Insoluble material was removed by centrifugation (113 000 g, 20 min), and the solubilized proteins were mixed with Nitrilotriacetic acid (NTA) agarose (equilibrated with 50 mM Tris/HCl pH 8.0, 5 or 10% glycerol, 300 mM KCl, 10 mM imidazole, 0.05% LDAO or 0.04% DDM) for 60 min. The loaded resin was packed onto a gravity flow chromatography column. During the following washing steps, the detergent in the buffer was exchanged to 0.04% DDM, and nonspecifically bound proteins were removed with 10 and 40 mM imidazole. 7His-SUMO-PvdT was eluted with 200 mM imidazole in 50 mM Tris/HCl pH 8, 300 mM KCl, 5 or 10% glycerol, and 0.04% DDM. PvdR6His was eluted from Ni-NTA with 400 mM imidazole in the same buffer. Protein concentrations were determined by a Bradford protein assay [23].

For downstream applications, the tag of 7His-SUMO-PvdT was removed. Hence, the protein was concentrated with a Proteus X-Spinner 2.5 Ultrafiltration Concentrator, and a HiTrap Desalting Column (Cytiva®, Marlborough, MA, USA) was used to exchange the buffer to 50 mM Tris/HCl pH 8, 300 mM KCl, 0.04% DDM, containing 5 or 10% glycerol. The protein was incubated overnight on ice

with Ulp protease. Thereby, the 7His-SUMO tag was removed, leaving PvdT without any tag. PvdT was separated from the remaining tag and the protease (which contains a histidine tag) using Ni-NTA magnetic beads (Genaxxon). For this purpose, the protein solution was incubated with the beads on a seesaw at 4 °C for 1 h. Afterwards, the magnetic beads binding Ulp and the 7His-SUMO tag were caught by a magnetic separator. The concentration of the remaining PvdT was again determined by Bradford quantification [23].

The purity of the proteins was estimated *via* Coomassie-stained SDS/PAGE, and the identity of the His-tagged proteins was analyzed by Western blotting using a mouse anti-6xHis (Invitrogen™, Waltham, MA, USA) or a mouse anti-5His (Qiagen, Hilden, Germany) primary antibody. A chicken anti-mouse alkaline phosphatase (AP)-conjugated antibody (Rockland, Limerick, PA, USA) was applied as a secondary antibody.

Surface plasmon resonance spectroscopy was performed with purified protein based on the protocol of Qasem-Abdullah *et al.* [24]. For this purpose, after purification of PvdR6His *via* ion exchange chromatography, size exclusion chromatography was applied, and buffer was subsequently exchanged against the running buffer, which contained 50 mM Tris/HCl pH 8.0, 300 mM KCl, 5% glycerol, and 0.04% DDM. For SPR analysis, the peak resulting in a molecular size of 98 kDa (peak C4) of the corresponding chromatogram was used. 7His-SUMO-PvdT was purified as described above. Buffer exchange was performed using a HiTrap™ desalting column (Cytiva®), and the 7His-SUMO tag was cleaved by Ulp overnight. Protein concentrations were determined using a Bradford protein determination technique [23].

Liquid chromatography–tandem mass spectrometry

In-gel digestion of proteins excised from SDS/PAGE with trypsin and desalting was performed as described [25]. Liquid chromatography–tandem mass spectrometry (LC–MS/MS) was performed on a nano-LC system (Ultimate 3000 RSLC, ThermoFisher Scientific, Waltham, MA, USA) coupled to an Impact II high-resolution Q-TOF using a CaptiveSpray nanoelectrospray ionization (ESI) source (MSBioLMU, Bruker Daltonics, Bremen, Germany). The nano-LC system was equipped with an Acclaim Pepmap nano-trap column (C18, 100 Å, 100 μm × 2 cm) and an Acclaim Pepmap RSLC analytical column (C18, 100 Å, 75 μm × 50 cm), both from Thermo Fisher Scientific. Peptides were separated over a 40 min linear gradient [5–37% (v/v) Acetonitrile, flow rate 250 nL min⁻¹]. MS1 spectra with a mass range from *m/z* 200–2000 were acquired at 3 Hz. The 18 most intense peaks were selected for MS/MS analysis using an intensity-dependent spectrum acquisition rate between 4 and 16 Hz. Dynamic exclusion duration was

0.5 min. Raw files were processed using the MAXQUANT software 2.0.3.1 with standard settings and digestion mode semi-specific free N-terminus [26].

Pyoverdine purification

For purification of pyoverdine for downstream applications, a protocol from Meyer *et al.* [27] was modified as follows: Strain *P. putida* KP1 was cultivated in CAA medium (0.5% casein hydrolysate, 6.77 mM K₂HPO₄, 1.01 mM MgSO₄·xH₂O) and grown at 30 °C with constant shaking for 16 h. Cells were removed by centrifugation (4500 g, 30 min), and the supernatant was filtered using a 0.2 µm PES filter and acidified to a pH of 6. Amberlite® XAD-4 (Alfa Aesar®) resin was used with a column volume of 2.5 × 10 cm·L⁻¹ of supernatant. The resin was washed with a methanol gradient from 0 to 50% to remove unwanted contaminants. Pyoverdine was eluted in fractions using 50% methanol. The solvent was removed, and pyoverdine was dissolved in 10 mM EDTA pH 6. EDTA was removed using a PD10 column packed with Sephadex G-25 (Cytiva®). The absorbance and fluorescence spectrum was measured (Fig. S1B), and the concentration of isolated pyoverdine was determined based on its absorbance at 400 nm using a molar extinction coefficient of 20 000 M⁻¹ cm⁻¹ [28].

Differential radial capillary action of ligand assay

For initial pyoverdine binding studies, the differential radial capillary action of ligand assay (DRaCALA) was used [29]. For this purpose, *P. putida* KT2440 Δ*pvdRT-opmQ* Δ*mdtA* was used to avoid binding of pyoverdine to the two encoded main pyoverdine transporters [12]. The strain was transformed with either pUCP20-ANT2-MCS [20] (control) or pUCP20-ANT2-7*His-SUMO-pvdT* (PvdT). Strains were grown until an OD₆₀₀ of 0.5, and gene expression was induced at 30 °C with 1 mM anthranilic acid for 3 h. Cells were harvested, resuspended in 50 mM Tris/HCl pH 8.0, and subsequently disrupted using two cycles of high pressure (1.35 kbar) and a Constant Systems Cell Disruptor. Afterwards, cell debris were separated (4500 g, 30 min), and membranes were harvested using ultracentrifugation at 235 000 g for 90 min. Membranes were resuspended in a small volume of 50 mM Tris/HCl pH 8.0. Every step was performed at 4 °C to avoid protein damage. Protein concentration was determined using a protocol by Peterson [22], and membranes were fast-frozen until usage. For dot-blot analysis, a final amount of 5 mg of membranes was applied to a dry nitrocellulose membrane (0.45 µm, Cytiva). Spots were dried and incubated with blocking solution [3% bovine serum albumin (BSA) in Tris-buffered saline (TBS)] for 30 min, and detection was performed with a primary mouse anti-5xHis and a secondary chicken anti-mouse AP-conjugated antibody. For DRaCALA experiments, total membrane protein was adjusted

to a range between 5.2, 8.8, 12.1, 14.9, 20.4, 22.7, and 25.2 mg·mL⁻¹, and a final concentration of 500 µM pyoverdine was added to each setup. Membranes were incubated for 10 min at room temperature (RT), and 5 µL were added to a dry nitrocellulose membrane (0.45 µm, Cytiva®) in duplicates resulting in drops with a final amount of 25.9, 43.9, 60.3, 74.4, 102.1, 113.4, or 126.0 µg, respectively. Drops were allowed to dry and were exposed in a BioRad Gel Doc XR+ Gel Documentation System using trans-UV light at a wavelength of 302 nm. Diffusion of the fluorescent ligand pyoverdine was evaluated using Fiji [30], the amount of the fraction bound ligand (*F_B*) was calculated according to the formula for *F_B*

$$= \left(\frac{I_{\text{inner}} - \left[A_{\text{inner}} * \left(\frac{I_{\text{total}} - I_{\text{inner}}}{A_{\text{total}} - A_{\text{inner}}} \right) \right]}{I_{\text{total}}} \right),$$

where *I_{inner}* is the fluorescence intensity of the inner circle, *I_{total}* the fluorescence intensity of the whole spot, *A_{inner}* the area of the inner circle, and *A_{total}* the area of the whole spot.

Data were plotted and analyzed using a nonlinear regression analysis with total (PvdT) and nonspecific (control) binding by GRAPHPAD PRISM 9.4.1 (GraphPad Software, San Diego, CA, USA). A minimum of three independent experiments was performed.

Surface plasmon resonance

Surface plasmon resonance spectroscopy assays were performed in a Biacore T200 device using a CM5 Series S carboxymethyl dextran sensor chips coated with His-antibodies from the Biacore His-capture kit (Cytiva®). Briefly, the chips were equilibrated with running buffer (50 mM Tris/HCl pH 8.0, 300 mM KCl, 5% glycerol, and 0.04% DDM) until the dextran matrix was swollen. After that, two flow cells of the sensor chip were activated using a 1 : 1 mixture of *N*-ethyl-*N*-(3-dimethylaminopropyl) carbodiimide hydrochloride and *N*-hydroxysuccinimide according to the protocol for standard amine coupling. For gaining a density of approximately 10 000 resonance units (RU) on the surface, a final concentration of 50 µg·mL⁻¹ anti-histidine antibody in 10 mM acetate buffer pH 4.5 was loaded onto both flow cells using a contact time of 420 s. Free binding sites of the flow cells were saturated by injection of 1 M ethanolamine/HCl pH 8.5. The sensor chip surfaces were prepared using a flow rate of 10 µL·min⁻¹. For interaction analysis, PvdR6His (0.5 µM) was captured onto one flow cell using a contact time of 200 s at a constant flow rate of 10 µL·min⁻¹. This resulted in a capture density of approximately 70–110 RU of PvdR6His. PvdT with five different concentrations (0.0625, 0.125, 0.25, 0.5, and 1 µM) was injected onto both flow cells performing single-cycle kinetics [31] using an association time of 120 s and a dissociation time of 600 s. The flow rate was kept constant at 30 µL·min⁻¹. The chip was regenerated after each cycle by removing PvdR6His entirely from the surface using 10 mM glycine pH 1.5 for 60 s at a flow rate of 30 µL·min⁻¹.

To test the influence of pyoverdine on complex formation between PvdR6His and PvdT, PvdT was incubated with either 0.1 mM pyoverdine or as a control with running buffer prior to injection. All experiments were performed at 25 °C. Sensorgrams were recorded using the BIACORE T200 CONTROL software 2.0.2 (Marlborough, MA, USA) and analyzed with the BIACORE T200 EVALUATION software 3.1. To acquire blank sensorgrams for the subtraction of the bulk refractive index background, the surface of flow cell 1 was not coated with PvdR6His. The baseline for the normalized referenced sensorgrams was set to 0. Peaks in the sensorgrams at the beginning and the end of the injection are due to the run-time difference between the flow cells for each chip. For the calculation of K_D values, steady state affinity curves were used, and the kinetics were fit, assuming a 1 : 1 binding model using the BIACORE T200 EVALUATION Software 3.1.

ATPase activity measurements

In order to determine the ATPase activity of PvdT, the release of inorganic phosphate during hydrolysis of ATP was recorded using a Malachite Green Phosphate Assay Kit (Sigma Aldrich® MAK307) similar as described [32]. Purified PvdT (0.2–0.4 μM) in 50 mM Tris/HCl pH 8, 300 mM KCl, 10% glycerol, 0.04% DDM, and 6 mM MgCl_2 was incubated in a 96-well plate at 30 °C with shaking (350 rpm). The reaction was started by the addition of ATP at given concentrations (0.1–3 mM), and incubation was continued for 20 min. To test whether purified PvdR6His affects the ATPase activity of PvdT, the adapter protein was added in 3-fold molar excess to the inner membrane protein (0.6–1.2 μM) before the start of the reaction with ATP. The influence of putative substrates on the ATPase activity was investigated by the addition of 10 or 100 μM PVD. The total volume of the individual reaction batches was 40 μL . After 20 min of incubation, the reactions were stopped by the addition of 10 μL of the malachite green solution, and for color development, the plate was further incubated at room temperature for 30 min. Afterwards, released inorganic phosphate was quantified at an absorbance of 620 nm in a Tecan infinite 200 pro plate reader. Controls for buffer, proteins, substrates, and ATP were performed in parallel. In addition, a phosphate standard was executed. The specific activity (v) was calculated as $\text{nmol P}_i \text{ mg}^{-1} \text{ PvdT min}^{-1}$ and ATPase activity was normalized to the amount of added PvdT (mg). For each condition, at least three independent experiments were performed and evaluated using GRAPHPAD PRISM version 9.4.1 and the Michaelis–Menten model ($v = V_{\text{max}} * [\text{ATP}] / (K_M + [\text{ATP}])$).

Statistical analysis and figure visualization

Data were plotted and statistically evaluated with GRAPHPAD PRISM version 9.4.1 for Windows, GraphPad Software, www.graphpad.com. Michaelis–Menten kinetic, one site—

total and nonspecific binding, unpaired *t*-test, and Dunnett's multiple comparisons test were performed as appropriate. AFFINITY DESIGNER version 1.10.4.1198 for Windows, Serif Ltd, Nottingham, UK, www.affinity.serif.com, was used for figure generation.

Results and Discussion

Pyoverdine binding properties of PvdT in membranes

PvdRT-OpmQ has been described as the main efflux system for matured and recycled pyoverdine in fluorescent *Pseudomonas* species [11,16]. Within this system, the inner membrane component PvdT is assumed to bind to substrates. Hence, the binding event has to take place in the periplasm, from where the substrates are pumped through PvdR and OpmQ into the environment. However, biochemical evidence for pyoverdine binding to PvdT has not been provided yet. For the initial analysis of a possible binding of pyoverdine to PvdT, a differential radial capillary action of ligand assay (DRaCALA) was performed following the protocol of Roeloffs *et al.* [29]. For this purpose, *pvdT* was expressed from plasmid pUCP20-ANT2-7His-SUMO-*pvdT* in *P. putida* KT2440 $\Delta pvdRT\text{-}opmQ\Delta mdT A$, and membranes were prepared. Membranes from cells transformed with the empty plasmid served as a negative control. Aliquots of membrane vesicles were incubated with 500 μM purified pyoverdine for 10 min. Subsequently, drops of membranes were placed on a nitrocellulose membrane. A dot-blot was performed to test whether the histidine-tagged protein was present in the membranes. As expected, the membranes of strain *P. putida* KT2440 $\Delta pvdRT\text{-}opmQ\Delta mdT A$ with the empty pUCP20-ANT2-MCS plasmid did not show a signal for PvdT (Fig. 1A), whereas for membranes prepared from cells transformed with pUCP20-ANT2-7H-SUMO-*pvdT*, incubation with an anti-5xHis antibody revealed the presence of the protein (Fig. 1B). The radius of diffusion of pyoverdine on nitrocellulose membranes was detected upon excitation of the fluorescent molecule by UV light (Fig. 1C,D). Thereby we found that pyoverdine spotted together with membranes containing PvdT was retained in part in the center of the spot (Fig. 1D). On the contrary, spotting of pyoverdine on nitrocellulose without *P. putida* membranes (Fig. 1C,D left drop), or with membranes without PvdT resulted in reduced fluorescent signals in the middle of the corresponding spots (Fig. 1C). Analysis of the bound pyoverdine fraction F_B using the formula from Roeloffs *et al.* [29] in dependence on the concentration of membranes resulted in a kinetic with a sigmoidal increase with higher membrane

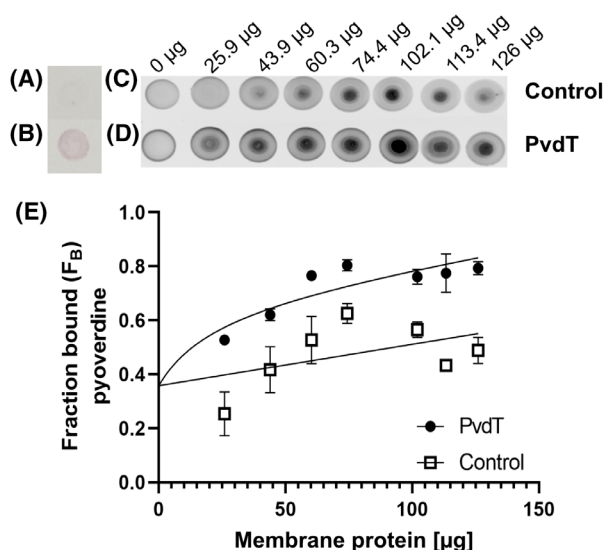


Fig. 1. Binding of pyoverdine to membranes harboring PvdT of *P. putida* KT2440. (A) Dot-blot of membrane vesicles containing no histidine-tagged protein (control) and (B) containing histidine-tagged PvdT. *P. putida* KT2440 $\Delta pvdRT\text{-}opmQ \Delta mdtA$ was transformed with either pUCP20-ANT2-MCS (control) or pUCP20-ANT2-7His-SUMO-pvdT (PvdT). The respective protein was expressed at an OD_{600} of 0.5 with 1 mM anthranilic acid for 3 h at 30 °C. Cells were washed with 50 mM Tris/HCl, pH 8.0, and disrupted during two cycles of high pressure (1.35 kbar) in a constant system cell disruptor, cell debris was separated and afterwards, membranes were harvested by ultracentrifugation at 235 000 *g* for 90 min. Membranes were resuspended in 50 mM Tris/HCl pH 8.0. For dot-blot analysis, a final amount of 5 mg of membranes was applied to a nitrocellulose membrane. Spots were dried and incubated with blocking solution (3% BSA in TBS) for 30 min, and detection was performed with a mouse anti-5xHis and a chicken anti-mouse AP-conjugated antibody. Membranes in 50 mM Tris/HCl pH 8.0 were incubated with a final concentration of 500 μ M pyoverdine for 10 min at RT. Drops of preincubated membranes with an increasing amount of total protein (25.9–126 μ g, left to right) were spotted on a nitrocellulose membrane and dried completely to perform a (C) DRaCALA assay of membranes containing no PvdT or (D) containing histidine-tagged PvdT. The first drop (left, C and D) represents the background without added membranes. Diffusion of fluorescence in the resulting spots was imaged using a BioRad Gel Doc XR+ Gel Documentation System (trans-UV 302 nm). (E) Spots of DRaCALA assay were quantified using Fiji [30], whereby the fraction bound (F_B) of pyoverdine was calculated as published in Roelofs *et al.* [29]. A nonlinear regression analysis with one site—total (PvdT) and nonspecific (control) binding analysis was performed using GRAPHPAD PRISM 9.4.1 and a minimum of three independent experiments. For illustration purposes, (C) and (D) show an inverted figure.

concentrations (Fig. 1E). Since the bacterial membrane, especially the Gram-negative membrane has a high abundance of negatively charged lipid head groups [33], unspecific binding of pyoverdine to the surface seems

possible. Alternatively, we cannot exclude the binding of pyoverdine to transporters that are not yet identified as being involved in siderophore secretion, as it has been discussed previously [12].

Purification of the inner membrane protein PvdT

To analyze the properties of PvdT in more detail, the protein was purified. In initial experiments, *pvdT* was expressed from plasmids pBAD24, pET16b, and pET21a in the *E. coli* strains BL21 (DE3) pLysS, C41, and C43. Western blotting with anti-His antibodies revealed either low levels of the ATP-binding cassette transporter (ABC transporter) in the membranes of the cells, or most of the protein were in the precipitate after low-speed centrifugation, suggesting the formation of insoluble protein aggregates. Therefore, we decided to express *pvdT* in *P. putida* KT2440 and derived strains from plasmids pSEVA224, pUCP-Nco, and pUCP20-ANT2-MCS. When *pvdT* was expressed from pSEVA224-10His and pUCP-Nco-10His, a large portion of the resulting protein was again in the precipitate after low-speed centrifugation. Finally, the 5' end of *pvdT* was fused to a sequence encoding a 7His tag, a SUMO signal sequence, and a glycine followed by a serine as a linker sequence. This construct was cloned into pUCP20-ANT2-MCS. Transformed with the resulting plasmid, the constitutive pyoverdine producer *P. putida* KP1 contained the highest levels of the corresponding protein in cytoplasmic membranes. Membranes containing 7His-SUMO-PvdT were solubilized with 1.5% LDAO. The solubilized protein was purified by Ni-NTA affinity chromatography (Fig. 2A,B). During chromatography, LDAO was replaced with 0.04% DDM. The procedure yielded approximately 0.4 mg of 7His-SUMO-PvdT from original 45 mg of total membrane protein using the pUCP20-ANT2-7His-SUMO-*pvdT* plasmid (Fig. 2C). The 7His-SUMO tag was removed by treatment with Ulp protease (~28 kDa). Subsequently, 7His-SUMO tag and Ulp protease were removed with magnetic Ni-NTA beads (Fig. 2A,B). The final yield of unlabeled PvdT was approximately 0.2 mg, starting from 45 mg of total membrane protein. The protein contamination at 28 kDa was from the Ulp protease, which was not entirely removed by the Ni-NTA bead treatment, as confirmed by Western blot analysis (Fig. 2A,B).

Purification of the adapter protein PvdR

PvdR contains an N-terminal twin-arginine pattern (TRRRLL) followed by a hydrophobic region of 21 amino acids (TATFIND-1.4 [34]) and a predicted

cleavage site between amino acid positions 34 and 35 (SignalP-6.0 [35]). The gene *pvdR* was cloned into pUCP20-ANT2-MCS, along with a nucleotide sequence encoding a 6His tag at the 3' end and expressed in *P. putida* KT2440. PvdR6His was detected in the membrane fraction but not in the soluble fraction (Fig. S2). Membranes were prepared and solubilized with 2% (w/v)

DDM. PvdR6His was purified by Ni-NTA affinity chromatography, reducing the concentration of detergent to 0.04% DDM. SDS/PAGE analysis of the resulting protein fractions revealed two protein bands at about 43 and 42 kDa (expected molecular weight of PvdR: 43 kDa; Fig. 2D). The protein of both bands was identified as PvdR6His by Western blotting (Fig. 2E)

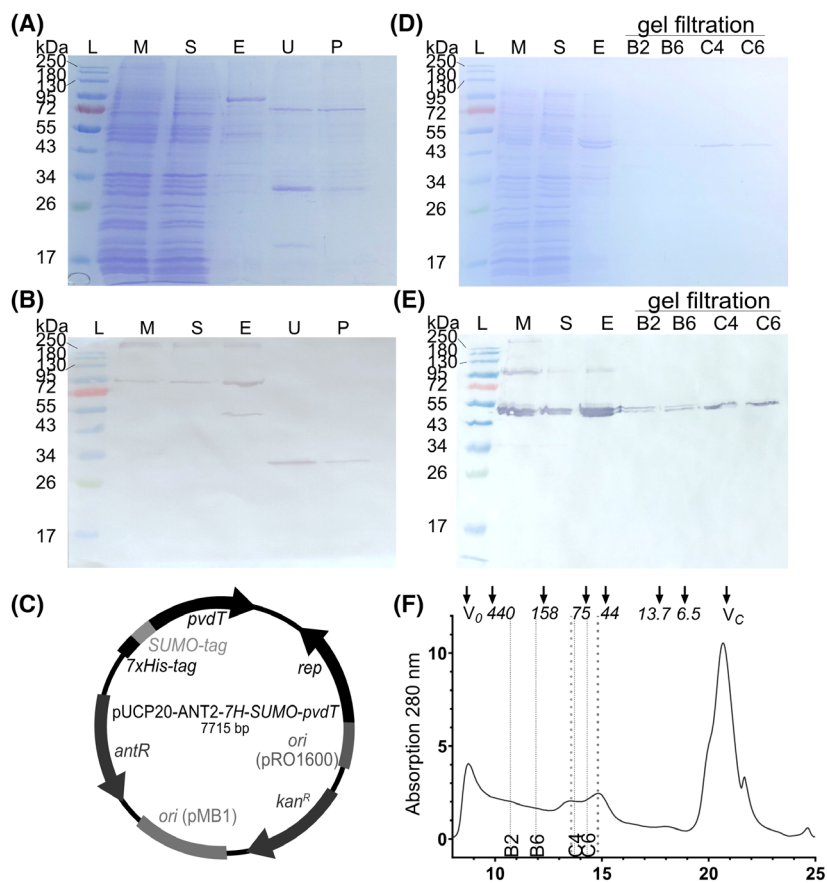


Fig. 2. Purification of inner and adapter proteins of the PvdRT-OpmQ efflux system. Respective genes were expressed in *P. putida* KT2440 and derived strains using pUCP20-ANT2-MCS [20]. The resulting protein was solubilized using 1.5% LDAO for 7His-SUMO-PvdT and 2% DDM for PvdR6His and purified by Ni-NTA affinity chromatography. (A) Coomassie-stained SDS/PAGE gel and (B) Western blot of the purification protocol steps for 7His-SUMO-PvdT (molecular weight 83 kDa, after Ulp cleavage: 70 kDa). (C) pUCP20-ANT2-7His-SUMO-pvdT derivative cloned for expression of PvdT. The SUMO tag was amplified from a pET-SUMO plasmid. (D) Coomassie-stained SDS/PAGE gel and (E) Western blot of steps of the purification protocol for PvdR6His (molecular weight 43 kDa). Protein was determined by the Bradford assay [23]. The P fraction of 7H-SUMO-PvdT yielded a protein concentration of 0.2 mg. For elution peak E of PvdR6His, a concentration of 0.2 mg was measured. Detection for (B) and (E) was performed using mouse anti-5xHis (Qiagen) as the primary antibody for PvdR6His (E) and mouse anti-6xHis (Invitrogen™) as the primary antibody for 7H-SUMO-PvdT (B). As a secondary antibody, a chicken anti-mouse AP-conjugated antibody (Rockland) was used for both proteins. L—protein standard; M—membranes; S—solubilisate; E—elution fraction of Ni-NTA chromatography; U—elution fraction with Ulp protease after second purification step with Ni-NTA beads; P—PvdT without 7H-SUMO tag and Ulp; B2/ B6/ C4/ C6—gel filtration fractions. (F) Size exclusion chromatography for the elution fraction E (D, E) for PvdR6His. Shown is a chromatogram for a Superdex200 column using a running buffer, containing 50 mM Tris/HCl pH 8.0, 300 mM KCl, 5% glycerol, and 0.04% n-dodecyl- β -D-maltopyranoside (DDM). Arrows are added to indicate the peaks for blue dextran (V_0 , void volume), ferritin (440 kDa), aldolase (158 kDa), conalbumin (75 kDa), ovalbumin (44 kDa), ribonuclease A (13.7 kDa), aprotinin (6.5 kDa), and acetone (V_C , geometric volume). Bold dotted lines indicate peaks corresponding to molecular weights of 98 and 55 kDa that probably represent dimeric and a monomeric PvdR6His with bound detergent. Thin dotted lines indicate the respective SEC fractions B2-C6 from the SDS/PAGE in (D) and the Western blot in (E).

and by LC–MS/MS (Table S4). Peptides of other proteins identified by LC–MS/MS represent minor impurities of the preparation. The Ni-NTA-based purification procedure yielded approximately 0.2 mg PvdR6His starting from 45 mg of total membrane protein. Blue native PAGE analysis showed that the protein occurs in various oligomeric states with molecular weights ranging from 132 kDa (trimer) to approximately 440 kDa (decamer or higher) (Fig. S3). Size exclusion chromatography (SEC) confirmed the tendency of PvdR6His to oligomerize. To work with a more defined protein fraction, PvdR6His of the peak corresponding to a molecular weight of 98 kDa (dimeric PvdR with bound DDM) was used (Fig. 2F). The stability and homogeneity of the dimer was not further investigated, which leaves open the possibility of the formation of higher oligomeric states.

To obtain more information on the identity of the two protein bands seen in the PvdR6His preparation after affinity chromatography and SEC (Fig. 2D,E), the bands at 43 and 42 kDa were excised and subjected to in-gel trypsin digestion and LC–MS/MS. An initial search revealed no peptides in any of the excised bands derived from the full-length N-terminal region of PvdR6His. It is possible that proteins are not fully digested by trypsin, which means peptides with variable cutting sites are generated. Since this is known to occur frequently in the N-terminal part of proteins, we could not identify the peptides in question with a conservative search for tryptic peptides. However, the search for semitryptically digested peptides with free N-terminus revealed a peptide in the range of amino acids 33 to 44, which was detected in the 43 kDa band but not in the 42 kDa band. Since the predicted

cleavage site is between positions 34 and 35 (Figs S4 and S5), we hypothesize that the 43 kDa band contains full-length PvdR6His while the 42 kDa protein band represents the protein without the predicted signal sequence (Tables S4 and S5). Interestingly, the TAT signal peptide can be found in *P. putida* and *P. parafulva* strains but not in the pathogen *P. aeruginosa* (Fig. S4). Especially in the region of the cleavage site (amino acids 32–36), the sequence is not conserved in homologous proteins of different pseudomonads (Fig. S5).

Pyoverdine influences the affinity of PvdT to PvdR6His *in vitro*

To test whether the inner membrane protein PvdT can bind its proposed substrate pyoverdine *in vitro* and unravel the molecular kinetics of this reaction, SPR measurements were performed using the single-cycle kinetic approach. The addition of pyoverdine to purified and immobilized PvdR did not yield a significant change in the SPR signal. However, the addition of the inner membrane component PvdT to immobilized PvdR6His led to a significant change in the mass of the protein complex that was reflected by the SPR signal (Fig. 3A). The dissociation constant (K_D value) for the interaction of PvdT and PvdR6His was determined with 27.7 ± 0.3 nM in the absence of pyoverdine. Next, we analyzed the possible impact of pyoverdine on the interaction between the two proteins. The results revealed an influence of pyoverdine on this interaction (Fig. 3B). Preincubation of PvdT with pyoverdine decreased the K_D value of the interaction of PvdT to PvdR6His to 4.35 ± 1.31 nM with a significance of 0.022 (P -value,

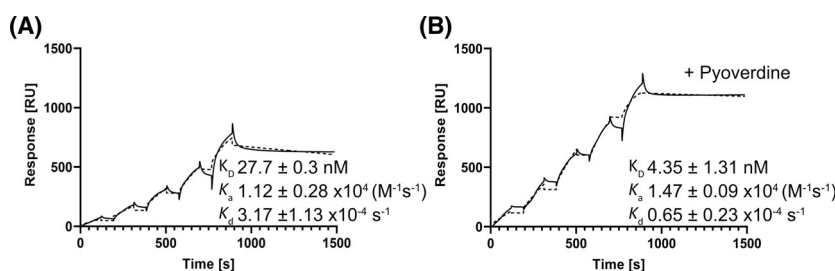


Fig. 3. Sensorgrams for the surface plasmon resonance (SPR) analysis of interactions of PvdT with immobilized PvdR6His under the influence of pyoverdine. (A) Sensorgrams for the interaction of PvdT with immobilized PvdR6His were obtained following a single-cycle kinetic. For analysis, PvdR6His was captured with a concentration of $0.5 \mu\text{M}$, and PvdT was applied as a ligand in a concentration range of $0.065\text{--}1 \mu\text{M}$. The response was recorded for 120 s during the association and 600 s for the dissociation phase. (B) Sensorgram for the interaction of PvdT preloaded with pyoverdine with immobilized PvdR6His. Here, PvdT was preincubated with $100 \mu\text{M}$ pyoverdine before application to SPR. The affinity towards PvdT increases significantly when PvdT is preincubated with pyoverdine (unpaired t-test, P -value = 0.022). For all measurements, proteins and ligands were dissolved in 50 mM Tris/HCl pH 8.0, 300 mM KCl, 5% glycerol, and 0.04% DDM. Graphs show representative data for one out of two biological replicates. Sensorgrams are plotted (solid line) and overlaid with a 1 : 1 global fit (dotted line) in each graph. The standard deviations result from calculating two independent biological replicates in the Biacore®.

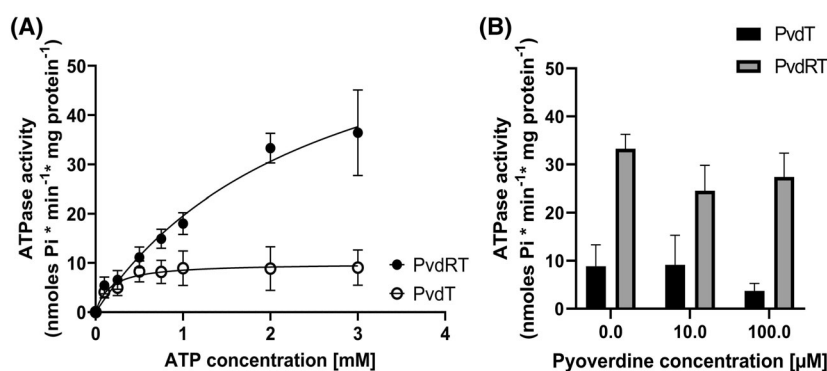


Fig. 4. PvdR regulates the ATPase activity of PvdT of *P. putida* KT2440. (A) Initial rates of inorganic phosphate (*P*) production by 0.2–0.4 μM PvdT in the absence (empty circles) or presence (filled circles) of 0.6–1.2 μM PvdR. Measurements were performed in 50 mM Tris/HCl pH 8, 300 mM KCl, 10% glycerol, 0.04% DDM, 6 mM MgCl_2 containing 0–3 mM ATP. *P*_i released from ATP was detected utilizing the Malachite Green Phosphate Assay Kit, Sigma Aldrich®. Michaelis–Menten parameters were calculated using the kinetic module of GRAPHPAD PRISM. In the absence of PvdR, PvdT had a very low ATPase activity with a $K_{\text{M(ATP)}}$ of 0.164 ± 0.07 mM and a $V_{\text{max(ATP)}}$ of 9.91 ± 0.95 nmol mg^{-1} min^{-1} . The addition of PvdR increased $K_{\text{M(ATP)}}$ to 2.58 ± 0.60 mM and $V_{\text{max(ATP)}}$ to 69.97 ± 9.50 nmol mg^{-1} min^{-1} . (B) Impact of pyoverdine on the ATPase activity of PvdT (black bars) and PvdRT (gray bars). Measurements were performed with 2 mM ATP and increasing amounts of pyoverdine in the given buffer. Pyoverdine did not have a significant impact on the ATPase activity based on an ordinary one-way ANOVA ($\alpha = 0.05$). Standard deviations were calculated using a minimum of three independent experiments.

unpaired *t*-test). The more than 6-fold decrease in K_{D} value in the presence of pyoverdine is mainly due to a decrease in the dissociation rate (OFF-rate, K_{d}) of PvdT from PvdR6His. In addition, the association rate (ON-rate, K_{a}) is slightly increased, indicating a faster association of PvdT-pyoverdine with PvdR6His than with PvdT alone. Taken together, the results demonstrate that pyoverdine physically interacts with the PvdT-PvdR6His complex and that this interaction favors a conformational change in the protein complex with enhanced stability. This conclusion is consistent with the result of the DRaCALA assay, which showed an enhanced interaction of pyoverdine with membranes containing PvdT compared to membranes without the protein (Fig. 1). Furthermore, the increase in the response units (RU) upon binding of PvdT-pyoverdine to PvdR6His suggests a 2 : 1 stoichiometry of PvdR to PvdT under these conditions (Fig. 3B). This is in accordance with the idea of an ABC transporter (PvdT) dimer interacting with an adaptor protein (PvdR) hexamer to form a functional transporter [14,36].

ATPase activity of PvdT

To further elucidate the enzymatic properties of purified PvdT, the ATPase activity was tested. For this purpose, initial rates of ATP hydrolysis (release of inorganic phosphate) were determined at ATP concentrations ranging from 0.1 to 3 mM. It is demonstrated that PvdT hydrolyzes ATP in the absence of substrate and PvdR, albeit at very low rates (Fig. 4A, Table 1).

The addition of purified PvdR stimulated the V_{max} value of the PvdT-dependent ATPase activity about sevenfold (P -value < 0.0001 , Tukey's multiple comparison test). The increase in $V_{\text{max(ATP)}}$ was accompanied by a 10- to 20-fold increase in the $K_{\text{M(ATP)}}$ value for ATP (Table 1, P -value 0.0014). Addition of the proposed ligand pyoverdine did neither significantly affect the ATPase activity of PvdT nor of the PvdRT complex (Fig. 4B). Nevertheless, $V_{\text{max(ATP)}}$ and $K_{\text{M(ATP)}}$ were slightly reduced (about 2-fold, P -values 0.0096) in the presence of pyoverdine (Table 1).

Following these results, the PvdR-induced increase in ATP hydrolysis rate at a given ATP concentration in our experiments was not due to an increased affinity of PvdT for ATP. On the contrary, because PvdR caused an increase in $K_{\text{M(ATP)}}$ by more than an order of magnitude, we hypothesize that PvdR stabilizes PvdT in a more functional structural arrangement, whereby the apparent lower affinity of PvdRT for ATP (higher $K_{\text{M(ATP)}}$) compared with PvdT may stimulate the turnover of the reaction cycle associated with ATP hydrolysis. Since intracellular ATP concentrations are expected to be in the lower millimolar range (*i.e.*, 0.5 to 10 mM [37]), the $K_{\text{M(ATP)}}$ value of 2.58 ± 0.60 mM of the PvdRT complex determined here suggests that ATP hydrolysis occurs between 10% and 100% of the maximum rate allowing cells to influence efflux activity depending on their energetic state. A stimulation of the ATPase activity of an inner membrane component by periplasmic adaptor proteins was originally shown for the MacAB-TolC efflux

Table 1. Kinetic parameters of the hydrolysis of ATP by PvdT. ATP hydrolysis by 0.2–0.4 μM PvdT in detergent solution (50 mM Tris/HCl pH 8, 300 mM KCl, 10% glycerol, 0.04% DDM, 6 mM MgCl_2) was analyzed in the presence and absence of 0.6–1.2 μM PvdR with or without 100 μM pyoverdine. ATP concentrations varied between 0.1 and 3 mM. Activity measurements were based on the detection of inorganic phosphate released from ATP using the Malachite Green Phosphate Assay Kit (Sigma Aldrich®). For statistical analysis, the ordinary one-way ANOVA ($\alpha = 0.05$) was performed. Comparison was performed with the following groups PvdT vs. PvdT + pyoverdine, PvdT vs. PvdRT, and PvdRT vs. PvdRT+pyoverdine. **P*-value < 0.05; ***P*-value < 0.005; *****P*-value < 0.0001. Mean values and standard deviations were calculated using protein from five independent preparations.

Protein	V_{max} [nmol ATP·min ⁻¹ ·mg ⁻¹ PvdT]	K_{M} (ATP) [mM]	k_{cat} [s ⁻¹]	$k_{\text{cat}}/K_{\text{M}}$ (ATP) [M ⁻¹ ·s ⁻¹]
PvdT	9.91 ± 0.95	0.164 ± 0.07	0.011 ± 0.002	81.34 ± 4.98
PvdT + pyoverdine	6.43 ± 0.67	0.064 ± 0.05	0.007 ± 0.001	133.23 ± 15.39
PvdRT	69.97 ± 9.50	2.58 ± 0.60	0.08 ± 0.018	33.60 ± 5.17
PvdRT + pyoverdine	40.41 ± 6.07	1.30 ± 0.42	0.05 ± 0.014	40.65 ± 8.57
Significance	PvdT-PvdRT**** PvdRT ± substrate**	PvdT-PvdRT**	PvdT-PvdRT**	PvdT-PvdRT* PvdT ± substrate**

system of *E. coli* [14,38]. Here, the periplasmic adapter protein MacA shows an overall identity of 37% to PvdR (Fig. S6), whereas the inner membrane protein MacB is about 45% identical to PvdT (Fig. S7).

The presence of a substrate to be exported (*e.g.*, pyoverdine) is another factor that is expected to influence the rate of ATP hydrolysis. While the observed pyoverdine-induced decrease in $K_{\text{M(ATP)}}$ can stimulate ATP hydrolysis at nonsaturating ATP concentration, $V_{\text{max(ATP)}}$ was not stimulated but even slightly reduced. Based on this result, we assume that substrate binding/transport and ATP hydrolysis are not tightly coupled under our experimental conditions. The ATPase activity of detergent-solubilized MacB of the MacAB-TolC efflux system from *E. coli* has also been shown to be insensitive to substrate [38]. In fact, many ABC transporters are notorious for having high levels of ATPase activity in the absence of their transportable substrate. This phenomenon is thought to maintain the transporter in an active state, enabling cells to react on suddenly occurring substrates immediately [39]. For MacAB, it has been observed that the interaction of MacA-MacB increases the rate of product release while the rate of ATP consumption decreases [14], which is consistent with the change in catalytic parameters we are showing. However, it cannot be excluded that the futile, wasteful expenditure of ATP is an artefactual consequence of the manipulation of detergent-solubilized proteins [13,40]. In any case, MacAB-TolC from *E. coli* couples substrate transport to ATP hydrolysis with high efficiency when reconstituted into nanodiscs [13].

Conclusion

In this study, the inner membrane ABC-type transporter PvdT and its periplasmic adapter protein PvdR of *P. putida* KT2440 were purified and biochemically characterized with respect to substrate binding and

ATPase activity. Binding assays with membranes and purified inner membrane protein PvdT provided biochemical evidence for a physical interaction of the protein with the siderophore pyoverdine. PvdT has a basal ATPase activity that is stimulated by PvdR. These results highlight that PvdRT-OpmQ indeed contributes to the pyoverdine cycle of *P. putida* KT2440.

Acknowledgments

Research in the group of HJ is supported by the Deutsche Forschungsgemeinschaft, projects JU333/6-1, and the Faculty of Biology, LMU Munich. We thank Prof. Thomas Brüser, Leibniz University Hannover, Germany, for kindly providing the pUCP20-ANT2-MCS plasmid, Alina Sieber for providing the pET-SUMO-yeiP plasmid, and Anna Litwuschuh for the generation of the pUCP20-ANT2-pvdR6His derivative. The graphical abstract was generated using BioRender.com. Open Access funding enabled and organized by Projekt DEAL.

Author contributions

NVS and HJ planned and supervised the experiments; NVS and ME generated the strains and plasmids; NVS performed the DRaCALA assay; NVS and ME purified proteins; ME performed ATPase activity measurements; SB performed SPR measurements; SS performed LC-MS/MS measurements and analysis; NVS and HJ wrote the manuscript; HJ supervised and acquired funding. All authors reviewed the results and approved the final version of the manuscript.

Data accessibility

Supporting data and findings of this study are available from the corresponding authors for a provable reason.

References

- Frawley ER and Fang FC (2014) The ins and outs of bacterial iron metabolism. *Mol Microbiol* **93**, 609–616.
- Cook-Libin S, Sykes EME, Kornelsen V and Kumar A (2022) Iron acquisition mechanisms and their role in the virulence of *Acinetobacter baumannii*. *Infect Immun* **90**, e0022322.
- Lasocki S, Gaillard T and Rineau E (2014) Iron is essential for living! *Crit Care* **18**, 678.
- Ringel MT, Dräger G and Brüser T (2016) PvdN enzyme catalyzes a periplasmic pyoverdine modification. *J Biol Chem* **291**, 23929–23938.
- Hider RC and Kong X (2010) Chemistry and biology of siderophores. *Nat Prod Rep* **27**, 637–657.
- Baune M, Qi Y, Scholz K, Volmer DA and Hayen H (2017) Structural characterization of pyoverdines produced by *Pseudomonas putida* KT2440 and *Pseudomonas taiwanensis* VLB120. *Biometals* **30**, 589–597.
- Pasqua M, Visaggio D, Lo Sciuto A, Genah S, Banin E, Visca P and Imperi F (2017) Ferric uptake regulator fur is conditionally essential in *Pseudomonas aeruginosa*. *J Bacteriol* **199**, e00472-17.
- Cornelis P, Matthijs S and Van Oeffelen L (2009) Iron uptake regulation in *Pseudomonas aeruginosa*. *Biometals* **22**, 15–22.
- Horiyama T and Nishino K (2014) AcrB, AcrD, and MdtABC multidrug efflux systems are involved in enterobactin export in *Escherichia coli*. *PLoS One* **9**, e108642.
- Hannauer M, Yeterian E, Martin LW, Lamont IL and Schalk IJ (2010) An efflux pump is involved in secretion of newly synthesized siderophore by *Pseudomonas aeruginosa*. *FEBS Lett* **584**, 4751–4755.
- Yeterian E, Martin LW, Lamont IL and Schalk IJ (2010) An efflux pump is required for siderophore recycling by *Pseudomonas aeruginosa*. *Environ Microbiol Rep* **2**, 412–418.
- Henriquez T, Stein NV and Jung H (2019) PvdRT-OpmQ and MdtABC-OpmB efflux systems are involved in pyoverdine secretion in *Pseudomonas putida* KT2440. *Environ Microbiol Rep* **11**, 98–106.
- Souabni H, Batista dos Santos W, Cece Q, Catoire LJ, Puvanendran D, Bavro VN and Picard M (2021) Quantitative real-time analysis of the efflux by the MacAB-TolC tripartite efflux pump clarifies the role of ATP hydrolysis within mechanotransmission mechanism. *Commun Biol* **4**, 493.
- Lin HT, Bavro VN, Barrera NP, Frankish HM, Velamakanni S, van Veen HW, Robinson CV, Borges-Walmsley MI and Walmsley AR (2009) MacB ABC transporter is a dimer whose ATPase activity and macrolide-binding capacity are regulated by the membrane fusion protein MacA. *J Biol Chem* **284**, 1145–1154.
- Crow A, Greene NP, Kaplan E and Koronakis V (2017) Structure and mechanotransmission mechanism of the MacB ABC transporter superfamily. *Proc Natl Acad Sci USA* **114**, 12572–12577.
- Imperi F, Tiburzi F and Visca P (2009) Molecular basis of pyoverdine siderophore recycling in *Pseudomonas aeruginosa*. *Proc Natl Acad Sci USA* **106**, 20440–20445.
- Chen WJ, Kuo TY, Hsieh FC, Chen PY, Wang CS, Shih YL, Lai YM, Liu JR, Yang YL and Shih MC (2016) Involvement of type VI secretion system in secretion of iron chelator pyoverdine in *Pseudomonas taiwanensis*. *Sci Rep* **6**, 32950.
- Ringel MT and Brüser T (2018) The biosynthesis of pyoverdines. *Microb Cell* **5**, 424–437.
- Yeterian E, Martin LW, Guillon L, Journet L, Lamont IL and Schalk IJ (2010) Synthesis of the siderophore pyoverdine in *Pseudomonas aeruginosa* involves a periplasmic maturation. *Amino Acids* **38**, 1447–1459.
- Hoffmann L, Sugue M-F and Brüser T (2021) A tunable anthranilate-inducible gene expression system for *Pseudomonas* species. *Appl Microbiol Biotechnol* **105**, 247–258.
- Wirtz L, Eder M, Brand AK and Jung H (2021) HutT functions as the major L-histidine transporter in *Pseudomonas putida* KT2440. *FEBS Lett* **595**, 2113–2126.
- Peterson GL (1977) A simplification of the protein assay method of Lowry et al. which is more generally applicable. *Anal Biochem* **83**, 346–356.
- Bradford MM (1976) A rapid and sensitive method for the quantitation of microgram quantities of protein utilizing the principle of protein-dye binding. *Anal Biochem* **72**, 248–254.
- Qasem-Abdullah H, Perach M, Livnat-Levanon N and Lewinson O (2017) ATP binding and hydrolysis disrupt the high-affinity interaction between the heme ABC transporter HmuUV and its cognate substrate-binding protein. *J Biol Chem* **292**, 14617–14624.
- Wang L, Leister D, Guan L, Zheng Y, Schneider K, Lehmann M, Apel K and Kleine T (2020) The *Arabidopsis* SAFEGUARD1 suppresses singlet oxygen-induced stress responses by protecting grana margins. *Proc Natl Acad Sci USA* **117**, 6918–6927.
- Cox J and Mann M (2008) MaxQuant enables high peptide identification rates, individualized p.p.b.-range mass accuracies and proteome-wide protein quantification. *Nat Biotechnol* **26**, 1367–1372.
- Meyer J-M, Stintzi A, de Vos D, Cornelis P, Tappe R, Taraz K and Budzikiewicz H (1997) Use of siderophores to type pseudomonads: the three *Pseudomonas aeruginosa* pyoverdine systems. *Microbiology* **143**, 35–43.
- Meyer JM and Abdallah MA (1978) The fluorescent pigment of *Pseudomonas fluorescens*: biosynthesis,

- purification and physicochemical properties. *Microbiology* **107**, 319–328.
- 29 Roelofs KG, Wang J, Sintim HO and Lee VT (2011) Differential radial capillary action of ligand assay for high-throughput detection of protein-metabolite interactions. *Proc Natl Acad Sci USA* **108**, 15528–15533.
- 30 Schindelin J, Arganda-Carreras I, Frise E, Kaynig V, Longair M, Pietzsch T, Preibisch S, Rueden C, Saalfeld S, Schmid B *et al.* (2012) Fiji: an open-source platform for biological-image analysis. *Nat Methods* **9**, 676–682.
- 31 Palau W and Di Primo C (2013) Simulated single-cycle kinetics improves the design of surface plasmon resonance assays. *Talanta* **114**, 211–216.
- 32 Abeyrathna N, Abeyrathna S, Morgan MT, Fahrni CJ and Meloni G (2020) Transmembrane Cu(I) P-type ATPase pumps are electrogenic uniporters. *Dalton Trans* **49**, 16082–16094.
- 33 Lin L, Chi J, Yan Y, Luo R, Feng X, Zheng Y, Xian D, Li X, Quan G, Liu D *et al.* (2021) Membrane-disruptive peptides/peptidomimetics-based therapeutics: promising systems to combat bacteria and cancer in the drug-resistant era. *Acta Pharm Sin B* **11**, 2609–2644.
- 34 Rose RW, Bruser T, Kissinger JC and Pohlschroder M (2002) Adaptation of protein secretion to extremely high-salt conditions by extensive use of the twin-arginine translocation pathway. *Mol Microbiol* **45**, 943–950.
- 35 Teufel F, Almagro Armenteros JJ, Johansen AR, Góslason MH, Pihl SI, Tsirigos KD, Winther O, Brunak S, von Heijne G and Nielsen H (2022) SignalP 6.0 predicts all five types of signal peptides using protein language models. *Nat Biotechnol* **40**, 1023–1025.
- 36 Fitzpatrick AWP, Llabrés S, Neuberger A, Blaza JN, Bai XC, Okada U, Murakami S, van Veen HW, Zachariae U, Scheres SHW *et al.* (2017) Structure of the MacAB-TolC ABC-type tripartite multidrug efflux pump. *Nat Microbiol* **2**, 17070.
- 37 Greiner JV and Glonek T (2021) Intracellular ATP concentration and implication for cellular evolution. *Biology (Basel)* **10**, 1166.
- 38 Tikhonova EB, Devroy VK, Lau SY and Zgurskaya HI (2007) Reconstitution of the *Escherichia coli* macrolide transporter: the periplasmic membrane fusion protein MacA stimulates the ATPase activity of MacB. *Mol Microbiol* **63**, 895–910.
- 39 Livnat-Levanon N, I. Gilson A, Ben-Tal N and Lewinson O (2016) The uncoupled ATPase activity of the ABC transporter BtuC2D2 leads to a hysteretic conformational change, conformational memory, and improved activity. *Sci Rep* **6**, 21696.
- 40 Orelle C, Mathieu K and Jault JM (2019) Multidrug ABC transporters in bacteria. *Res Microbiol* **170**, 381–391.

Supporting information

Additional supporting information may be found online in the Supporting Information section at the end of the article.

Fig. S1. Structure and absorbance spectra of pyoverdine of *P. putida* KT2440.

Fig. S2. Western blot testing the localization of PvdR6His cell fractions of *P. putida* KT2440 strains.

Fig. S3. Electrophoretic analysis of purified PvdR6His and PvdT.

Fig. S4. Alignment of PvdR of *P. putida* KT2440 and related pseudomonads.

Fig. S5. Sequence logo frequency plot for amino acids 31 to 37 of PvdR in different pseudomonads.

Fig. S6. Alignment of PvdR of *P. putida* KT2440 and MacA of *E. coli* K12.

Fig. S7. Alignment of PvdT of *P. putida* KT2440 and MacB of *E. coli* K12.

Table S1. Strains used in this investigation.

Table S2. Plasmids used in this investigation.

Table S3. Oligonucleotides used in this investigation.

Table S4. List of all proteins identified in the SDS/PAGE of purified PvdR6His by LC–MS/MS.

Table S5. List of all peptides identified for PvdR6His in the 43 and 42 kDa band using LC–MS/MS.